Pressure Control in Minimally Invasive Surgery

Van Muot Nguyen, Institute of Automation, University of Rostock
Email: van.nguyen@uni-rostock.de
Torsten Jeinsch, Institute of Automation, University of Rostock

Abstract

In the field of minimally-invasive surgery (MIS), double roller pump is one of the medical therapy devices which have been used as an effective method for controlling the rinsing fluid [1]. For example in the knee arthroscopy, the pressure inside the joint of the knee needs to be controlled during the operation time. The stability of the pressure takes a central role in this case because this avoids the situations of hemorrhages and fluid depletion [2, 3, 4]. In this paper, a double roller pump is used as a medical device for controlling the pressure in the knee arthroscopy. The pressure inside the knee joint is influenced by the actual flow of the rinsing fluid. The operation of the process was simulated and linearized for controller design. A physical model of the knee joint was built for the experiments. The PI controller was designed based on Symmetric Optimum (SO) method with an anti-windup strategy. Some parameters of the controller were adjusted, and the results were compared in both simulation and real-time experiment. The adjustments of phase margin in frequency domain were used for analyzing and evaluating the effectiveness of the double roller pump usage in minimally invasive surgery.

1 Introduction

Double roller pump (DRP) is now applied commonly in minimally-invasive surgery. For the visibility and accessibility in the operative area, the liquid is used for flushing via trocars. It is necessary for a surgeon in controlling the pressure inside the area of operation during MIS. Before the usage of automatic pump systems, gravity flow method was used first because of the simplification in setup procedure [4,5]. From gravity flow method, the pressure is controlled via the inflow of fluid. This was made by changing the height of the fluid bag. However, this resulted in some troubles because of the inconvenience and inaccuracy. Since the years of the 1970s, types of automatic pump system have been developed for pressure and flow control [4]. A single roller pump was used for pressure control via inflow of fluid only. So far, DRP has been used for controlling the pressure as well as the inflow and outflow separately. In this contribution, DRP is used for the replacement of gravity flow method or single roller pump type. Our focus is to build a process in experiments and design a controller of pressure via the flows of fluid in arthroscopy. This is a case of studies for pressure control using DRP in MIS.

The pressure inside the closed operation area is changed rapidly depending on the change of the liquid flow in minimally-invasive surgery. Applying in a typical procedure of the knee joint arthroscopy, the pressure inside the joint needs be controlled for more accuracy to the desired value whenever there is some change of liquid flow. This avoids unwanted situations harmful to the patients. This type of automatic control provides to the surgeons an easier way of using medical device. So the waste time for initial parameters setup as well as the operation time will be reduced effectively.

An overview of the system operation is simplified in Figure 1 [6]. One roller pump is used for providing the liquid inflow, and another roller pump is used for the liquid outflow. From the simulation in Matlab Simulink, the process was linearized via the step response output. The linearized transfer function consists of a first-order form and an integrating term. The controller of the process is designed with a PI controller based on the symmetrical optimum method with the anti-windup algorithm [7-10]. Some more details of the system overview are described in section 2. The controller design is presented in section 3. Section 4 is the content of experimental results and discussion. Finally, the conclusion is summarized in section 5.

2 System Overview

As shown in Figure 1, the controlled process includes the DRP with two DC motors for pumping the fluid in and out from the operation area in MIS; two pressure sensors for the pressure measurements. These measured data are calculated to the inflow Q_{in} and the outflow Q_{out}. Two flexible rubber tubes are used for connecting from the rinsing fluid container via the DRP to the operation region which is considered to the knee joint. Another pressure sensor is used to measure the actual pressure inside the knee joint model. While doing experiments on the real patient are unacceptable because of the risks, a plastic ball as a reservoir was used for a knee joint model in arthroscopic surgery.

One DC motor (called M1) is used together with a roller pump for controlling the inflow of rinsing fluid to the operation area of the knee joint. Another DC motor (called M2) is used with another roller pump for activating the fluid out from the operation area. The outflow can be adjusted whenever needed by a surgeon. The inflow should be controlled automatically corresponding to the outflow. This means that the controller needs to be designed for keeping the pressure in the joint knee model close to the desired value. For the knee arthroscopy, the range of reference pressure is suggested from 30 to 60mmHg over the ambient pressure [4, 12], (30mmHg is approximate to 4000 Pa).

From the experiments on the physical model, the step response outputs of the two motors M1 and M2 were identified. Equation (1) is the linear function of the motors used as the first order form with the time constant T and the delay time τ.

$$G_M(s) = (\mathrm{e}^{-\tau \cdot \mathrm{s}}) \cdot \frac{\mathrm{K}_M}{\mathrm{T} \cdot \mathrm{s} + 1} \tag{1}$$

Where: K_M is a constant.

For modeling the operation of the double roller pump, it can be assumed that the liquid flow from the pump Q_{pump} is depended on the rotary speed of the motor ω_M.

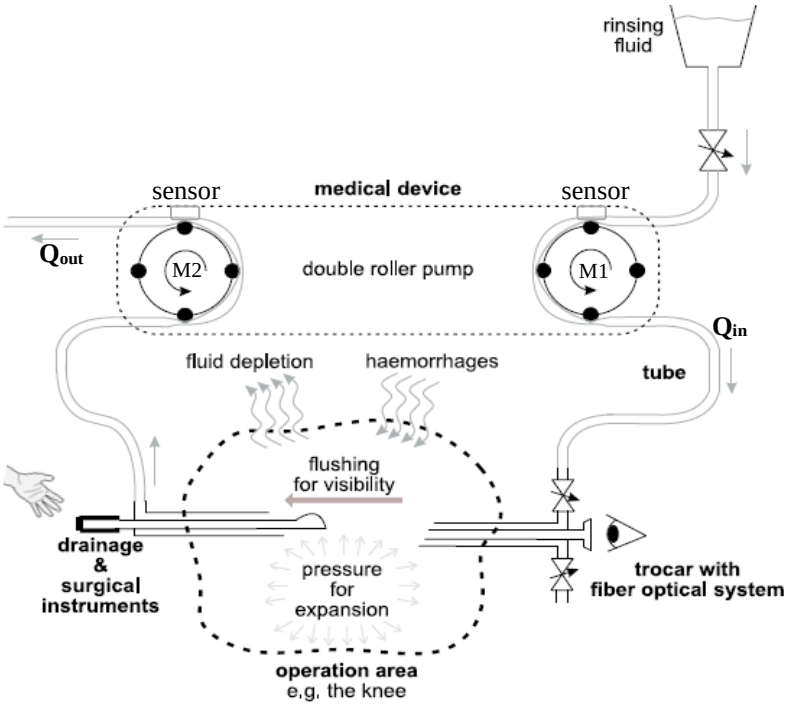

Figure 1: An overview of the knee arthroscopy in MIS [6]

$$Q_{pump} = f(\omega_M) \tag{2}$$

Due to the hydraulic capacity C_{hyd} of the tube, a part of the flow generated by the pump still remains in the tube. This part is called $\Delta Q_{tube} = Q_{pump} - Q_{tube}$. This causes the delay of pressure change at the end of the tube close to the pump. The relationship is indicated in equation (3).

$$\dot{p}_{pump} = \frac{Q_{pump} - Q_{tube}}{C_{hyd}} = \frac{\Delta Q_{tube}}{C_{hyd}} \tag{3}$$

With C_{hyd} is a constant; Q_{pump} and Q_{tube} are the flows.

In addition, the flow in the tube Q_{tube} is a nonlinear component depending on the pressure changed in the tube. This change of pressure is $\Delta p_{tube} = p_{pump} - p_{res}$ (p_{pump} and p_{res} are the pressure from the pump and the pressure from the reservoir respectively).

$$Q_{tube} = f(\Delta p_{tube}) \tag{4}$$

For modeling of the knee joint in MIS, a reservoir was used with the constant volume V_{res}. The value V_{res} equals to the sum of air volume V_{air} and liquid volume V_{liq}.

$$V_{res} = V_{knee} = V_{air} + V_{liq} = constant \tag{5.a}$$

$$V_{air}(t) = V_{res} - V_{liq}(t) \tag{5.b}$$

Any change of the liquid volume (dV_{liq}/dt) inside the reservoir leads to the change of air volume (dV_{air}/dt), but in negative sign.

$$\dot{V}_{air}(t) = -\dot{V}_{liq}(t) \tag{6}$$

The volume of liquid V_{liq} in the reservoir is changed by the actual change of liquid flow $Q_{res} = Q_{in} - Q_{out}$. This volume is described in equation (7).

$$V_{liq}(t) = V_{liq0} + \int_0^{V_{res}} Q_{res} dt \tag{7}$$

Where: V_{liq0} is the initial volume of liquid in the reservoir (It is assumed to a constant).

Then the equation (7) can be rewritten as in (8).

$$\dot{V}_{liq}(t) = Q_{res}(t) \tag{8}$$

On the other hand, by considering the air inside the reservoir as an ideal gas, the equation of the pressure from the ideal gas law is written as in (9).

$$p_{res}(t) \cdot V_{air}(t) = m_{air} \cdot R \cdot T_{air} \tag{9}$$

Or:

$$p_{res}(t) = \frac{m_{air} \cdot R \cdot T_{air}}{V_{air}(t)} \tag{10}$$

Where: p_{res}: is the pressure in the reservoir (it is also called p_{knee}).

V_{air} and m_{air} are the volume and the mass of the gas in the reservoir respectively.

R: is the ideal gas constant; T_{air}: is the absolute temperature of the gas.

It can be assumed that the values of m_{air} and T_{air} in the reservoir are not changed even if the pressure or the volume of gas is changed. So the equation (10) can be transformed into (11).

$$\dot{p}_{res}(t) = -\frac{(m_{air} \cdot R \cdot T_{air}) \cdot \dot{V}_{air}(t)}{(V_{air}(t))^2} \tag{11}$$

By substituting the equations (6), (8) and (10) into (11), the equation is rewritten as (12) which indicates the nonlinear formation of the process.

$$\dot{p}_{res}(t) = -\frac{p_{res} \cdot \dot{V}_{air}(t)}{V_{air}(t)} = \frac{p_{res} \cdot Q_{res}(t)}{-\int_0^{V_{res}} Q_{res}(t) dt} \tag{12}$$

The modelling of the whole process was implemented in Matlab Simulink using parameters in Table 1. From the step response output, the process was linearized. The transfer function of the process is described in equation (13), which includes a first-order form, an integrating component and a function of the delay time τ.

$$G(S) = (e^{-\tau \cdot s}) \cdot \frac{1}{s} \cdot \frac{K}{(\mathrm{T} \cdot \mathrm{s} + 1)} \tag{13}$$

Where: $\tau = 0.006$ (sec), is the delay time; $T = 0.038$ (sec) is the time constant.

K = constant.

Name	Value	Unit	Description
V_{res}	0.002	m^3	Total volume of the reservoir
V_{liq0}	0.001	m^3	Initial liquid volume in the reservoir
p0	101325	Pa	Ambient pressure (≈760mmHg)
C_{hyd}	10^{-11}	m^3 / Pa	Capacity of the tube being used

Table 1: Parameters used for simulation and experiment

3 Controller Design

The pressure in the reservoir needs to be controlled via the rotary speed of the two motors together with the DRP for activating the flows of fluid. The block diagram of the closed loop control of the process is illustrated in Figure 2.

The plant G(s) in Figure 2 is considered to the linearized process in (13). The main input of the controller is the error between the reference pressure p_{ref} and the measured pressure p_{res} from the output of the process. Another input of the controller $u_2(t)$ is activated from a surgeon like a disturbance to the system. The signal $u_1(t)$ is generated from the controller $G_c(s)$ for control the process G(s). The goal is to ensure the output pressure p_{res} close to the desired value of p_{ref}. It should be noted that the signal $u_1(t)$ is used to activate the motor M1 for control the inflow, and the signal $u_2(t)$ is used to activate the motor M2 for the outflow.

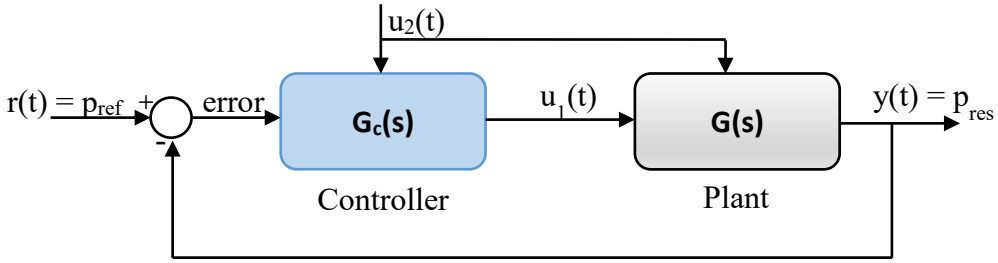

Figure 2: A closed loop of the controlled process

- **PI controller design**

With the linearized process indicated in (13), a controller is suggested as a PI controller based on symmetric optimum method [7, 8, 9]. A general PI controller is described in (14.a).

$$G_c(s) = K_P + \frac{K_I}{s} = K_P\left(1 + \frac{1}{T_I \cdot s}\right) \quad (14.a)$$

Equation (14.b) is the description of the PI controller based on SO method [7, 8, 9, 10].

$$G_c(s) = K_c \frac{(T_N \cdot s + 1)}{T_N \cdot s} \quad (14.b)$$

Comparing from (14.a) and (14.b): the gain $K_c \equiv K_P$; the integral time $T_N \equiv T_I$. The transfer function of the process in open-loop control $G_{OL}(s)$ is written by (15).

$$G_{OL}(s) = G_c(s) \cdot G(S) = (e^{-\tau \cdot s}) \cdot (\frac{K \cdot K_c}{T_N}) \cdot \frac{1}{s^2} \cdot (T_N \cdot s + 1) \cdot \frac{1}{(\mathrm{T} \cdot \mathrm{s} + 1)} \quad (15)$$

The parameters T_N and K_C are calculated by the equations (16), (17) and (23). In the SO method, the maximal phase response is adjusted at the crossover frequency (ω_c) of the open loop controlled process. In addition, the Bode phase diagram of (15) is symmetrical around the crossover frequency [8, 11]. Characteristics of the plant G(s) and the open-loop controlled process (15) are illustrated in Figure 3.

The integral time:

$$T_N = a^2 \cdot T \; ; \qquad \text{(with a > 1)} \tag{16}$$

Where the parameter 'a' is depended on the desired phase margin φ_R.

$$a = \frac{1 + sin(\varphi_R)}{cos(\varphi_R)} \tag{17}$$

The phase margin φ_R of the process with the controller is calculated from [8, 13] in (18).

$$\varphi_R = \pi + \varphi(\omega_c) = \tan^{-1}(T_N\omega_c) - \tan^{-1}(T\omega_c) \tag{18}$$

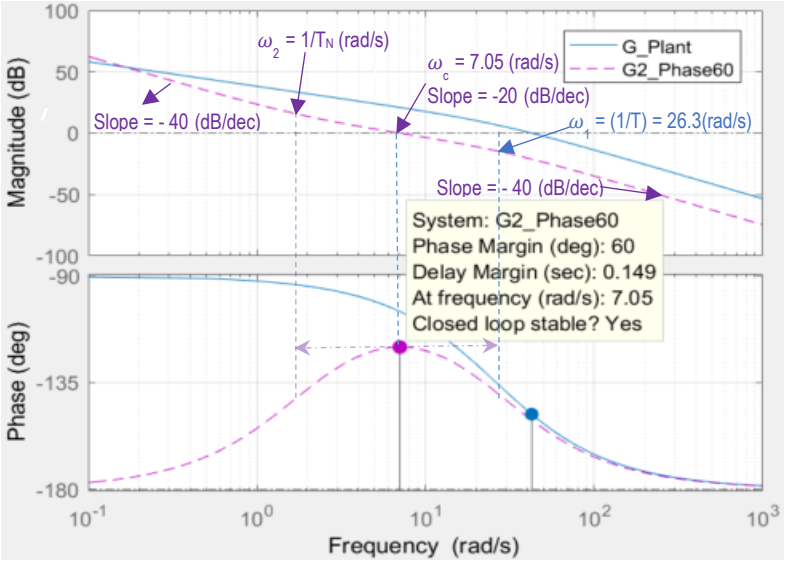

Figure 3: Bode diagram of the plant G(s) and the open-loop controlled process $G_{OL}(s)$.

The integral time T_N and parameter 'a' are calculated depending the desired value of φ_R.

For the gain value K_C of the controller in (14), it can be calculated from the condition of magnitude in (19).

$$M(G_{\mathrm{OL}}(\mathrm{j}\omega_c)) = 1 \tag{19}$$

$$\Leftrightarrow \frac{K \cdot K_C}{T_N}\left(\frac{1}{(\omega_c)^2}\right)\left(\frac{\sqrt{(\mathrm{T}_N \cdot \omega_c)^2+1}}{\sqrt{(\mathrm{T} \cdot \omega_c)^2+1}}\right) = 1 \tag{20}$$

On the other hand, when taking derivation by $\omega = \omega_c$ from (18), it is written in (21).

$$\frac{d(\varphi_R)}{d(\omega)}\Big|_{\omega=\omega_c} = \frac{T_N}{1 + (T_N \cdot \omega_c)^2} + \frac{-T}{1 + (T \cdot \omega_c)^2} = 0 \tag{21}$$

Definitely, with T ≠ T_N, the crossover frequency in equation (21) is solved as in (22).

$$\omega_c = \frac{1}{\sqrt{T_N \cdot T}} \tag{22}$$

By substituting (16) and (22) into (20), the gain of the controller Kc is solved in (23).

$$K_C = \frac{1}{a \cdot K \cdot T} \tag{23}$$

It is clear that both the parameters K_C and T_N of the PI controller will be altered when the phase margin φ_R is changed.

- **Anti-windup for PI controller**

The controller $G_C(s)$ in Figure 2 is used to control the roller pump via the DC motor M1. The input voltage limitation of the motor is from 0 to 5 VDC. To limit the wind-up phenomenon which is usually taken into account in PID controllers using with an integral term of the nonlinear process [8], an anti-windup algorithm was added in the PI controller as shown in Figure 4. In this method, the integrating part stops working when the output of the controller is out of the voltage range used for the motors. This means that when the control signal $u_1(t)$ is higher than 5 VDC or less than 0 VDC, the output signal from logical operator OR becomes a high logic. This high logic signal makes the integrator stop working. Otherwise, the integrator works normally. The step response of the closed-loop controlled process is shown in Figure 5.

When the process (13) is considered to the formula of (24) by ignoring the very small delay time τ, then the damping coefficient ζ should be chosen equal or greater than 0.5 in order to keep the controlled process stable [14].

$$G(S) = \frac{1}{s} \cdot \frac{K}{(\mathrm{T} \cdot \mathrm{s} + 1)} = \frac{1}{s} \cdot \frac{\omega_0^2}{(\mathrm{s} + 2\zeta\omega_0)} \tag{24}$$

Where: $\omega_0 > 0$ is the natural frequency, and $\zeta > 0$ is the damping coefficient.

The closed-loop control transfer function of the system can also be approximated to the second-order form for controller design. Depending on the phase margin, the parameters of the controller and the overshoot of the controlled process in Simulink are shown in Table 2.

Phase margin φ_R (degree)	**Gain K_C**	**Integral time T_N (sec)**	**Parameter a**	**Settle time/Overshoot (sec / %)**	**Crossover frequency ω_c (rad/s)**
37° (ζ ≈ 0.5)	0.2412	0.1529	2	0.60 / 49.80	13.1
45° (ζ = 0.707)	0.1341	0.2215	2.414	0.70 / 36.80	10.9
50.69° (ζ = 0.9)	0.1156	0.2979	2.8	0.75 / 29.40	9.4
53.13° (ζ = 1)	0.1079	0.342	3	0.80 / 26.90	8.77
60° (ζ > 1)	0.0867	0.5293	3.732	1.00 / 19.95	7.05
78° (ζ > 1)	0.034	3.4399	9.514	3.40 / 7.60	2.77

Table 2: Parameters from PI controller in different cases of phase margin

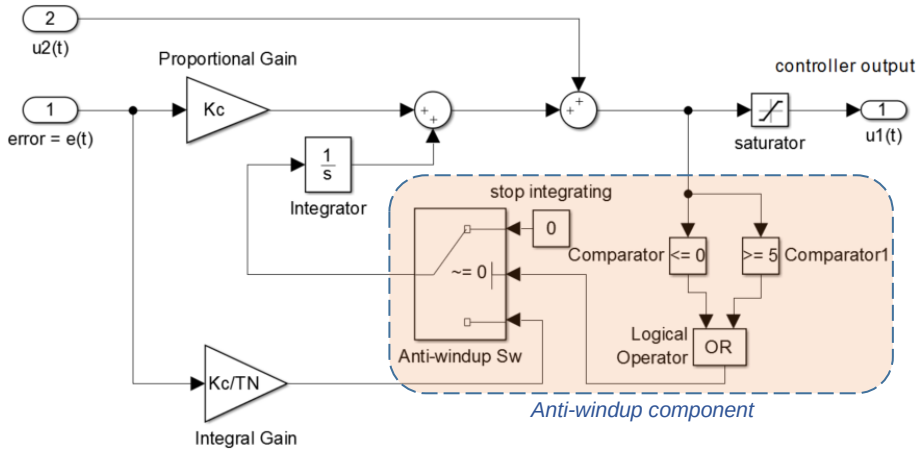

Figure 4: An anti-windup algorithm for the designed PI controller

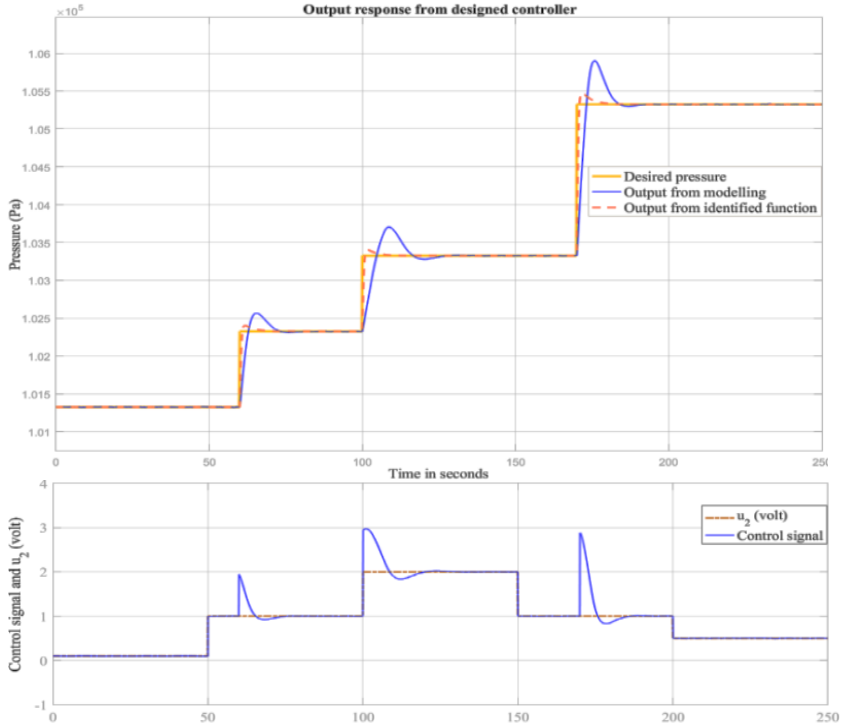

Figure 5: Step response from the designed controller on Simulink (phase margin = 78°)

4 Results and Discussion

Some experiments were implemented with different parameters of phase margin. Each of the chosen phase margin in the frequency domain, the parameters of the controller were calculated respectively. From the three cases comprarison of Bode diagrams in Figures 6, it should be mentioned that the integral time of T_N is increased when the phase margin is increased. And therefore the crossover frequency is adjusted decreasingly. In other words, the bandwidth of the controlled process is expanded relatively into a lower frequency area by increasing the phase margin. The main point of the controller is to keep the phase response symmetrical around the crossover frequency but also reduce the steady-state error. So T_N value must be greater than the time constant T of the process. Three cases of experimental results with different phase margin are presented in Figures 7.a, 7.b and 7.c.

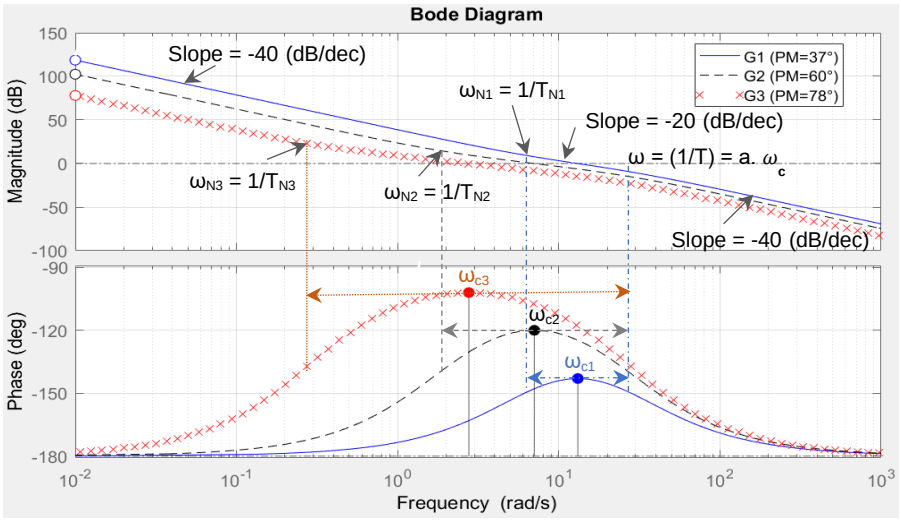

Figure 6: Bode diagram of the open-loop controlled process $G_{OL}(s)$ in 3 cases of phase margin

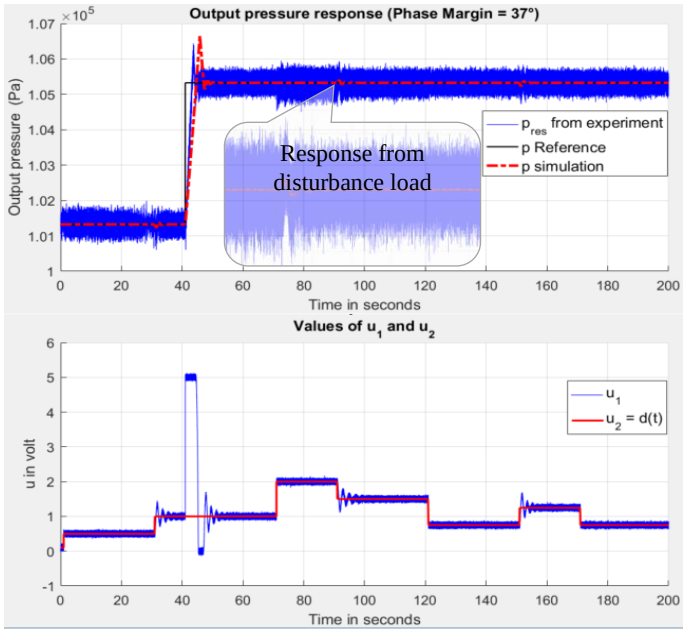

Figure 7.a: Experimental result in case of φR = 37°

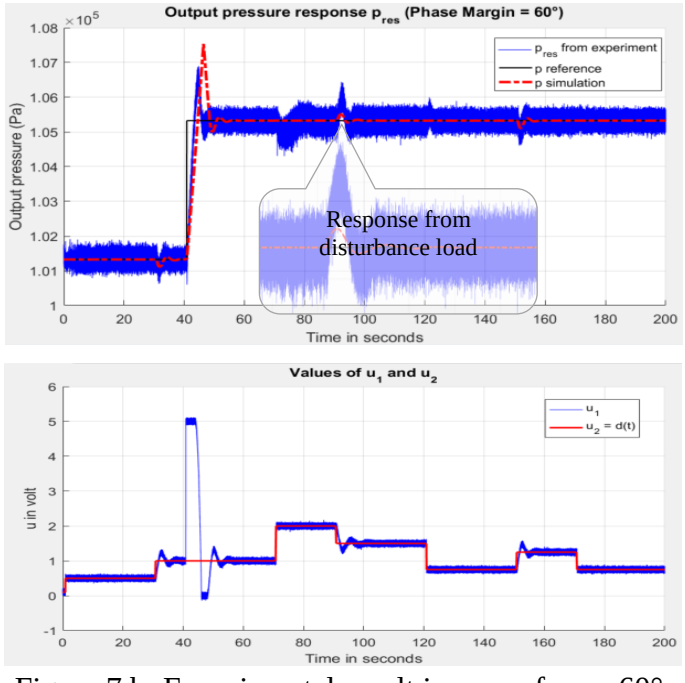

Figure 7.b: Experimental result in case of $\varphi_R = 60°$

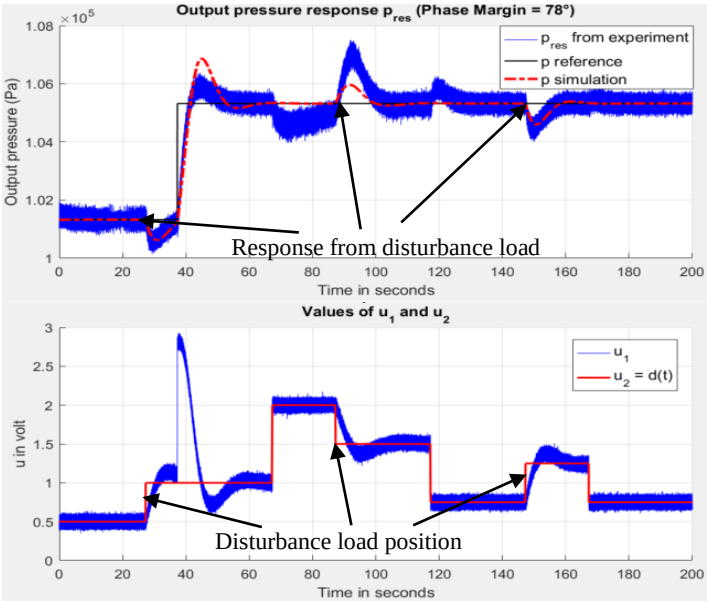

Figure 7.c: Experimental result in case of φ_R =78°

From the results in Figures (7.a, 7.b and 7.c), the measured output pressure was controlled close to the desired value of 30mmHg above to the ambient pressure p_0 (total value is approximate to 105325 Pa). Noting that the more increased phase margin is, the more decreased overshoot is. However, the more decreased phase margin is, the more reduced settling time is. For the goal of controller design with the preferred overshoot less than 20%, it would be better to choose the phase margin between the values 60° and 78°.

5 Conclusion

In this contribution, an overview of the knee arthroscopy in MIS was introduced, and the medical device DRP was used in experiments for pressure control via the flows of fluid. With the phase margin of 37°, the typical case of the symmetric optimum method from Kessler's [14, 15], the settling time was reduced fastly but the overshoot was more than 43%. By increasing the phase margin up to 78°, the overshoot was reduced gradually down to 7.6% while the settling time was taken longer to 3.4 seconds on simulation of linearized function. However, the good point is that the system was stable with some unknown disturbance loads from the input of the two motors. This result would be suitable for implementing to the real patient in MIS, especially in the knee joint arthroscopy. But for a wide application to other operating areas of the patient's body, the system should be developed with some more functions so that it can be used with different cases of minimally invasive surgery. For example, basing on the current blood pressure on the specific patient, the system can be controlled and adapted to the states of blood pressure and other suitable requirements automatically.

6 References

[1] R., Bergstrom; J., Gillquist: The Use of an Infusion Pump in Arthroscopy, The Journal of Arthroscopic and related Surgery, pp. 41-45, Arthroscopy Association of North America, 1986.

[2] G. J. M. Tuijthof; M. M. de Vaal; I. N. Sierevelt; L. Blankevoort; M. P. J. van der List, Performance of Arthroscopic Irrigation Systems Assessed with Automatic Blood Detection, in Knee Surgery Sports Traumatology Arthroscopy, Vol.9, pp. 1948-1954, 2011.

[3] Chang, Dwayne; P.Manecksha, Rustom; Syrrakos Konstantinos; and Lawrentschuk Nathan: An Investigation of the Basic Physics of Irrigation in Urology and the Role of Automated Pump Irrigation in Cystoscopy, The Scientific World Journal, Article ID 476759, 2012.

[4] S. Hsiao, Mark; Kusnezov, Nicholas; N. Sieg Ryan; D. Owens Brett; P. Herzog Joshua: Use of an Irrigation Pump System in Arthroscopic Procedures, in Orthopedics, 2016.

[5] Muellner, Thomas; A., Menth-Chiari Wolfgang; Reihsner, Roland; Eberhardsteiner, Josef; and Engebretsen, Lars: Accuracy of Pressure and Flow Capacities of Four Arthroscopic Fluid Management Systems, The Journal of Arthroscopic and Related Surgery, Vol.17 -No. 7, pp. 760-764, Arthroscopy Association of North America, 2001.

[6] Smolinski, Eike; Benkmann, Alexander; Westerhoff, Peter; Nguyen, Van Muot; Drewelow, Wolfgang; Jeinsch, Torsten: A Hardware-In-The-Loop Simulator for the Development of Medical Therapy Devices, 20th IFAC World Congress, France, 2017.

[7] Aström, Karl J.; and Hägglund, Tore: Advanced PID control, ISA - Instrumentation, Systems, and Automation Society, 2006.

[8] Aström, Karl J.; and Hägglund, Tore: PID controller: Theory, Design, and Tuning, 2nd Edition - Instrument Society of America, 1995.

[9] Otto, Föllinger: Regelungstechnik - 11 Auflage, VDE Verlag GmbH, 2013.

[10] Lutz, Holger; und Wend, Wolfgang: Taschenbuch der Regelungstechnik, Verlag Harri Deutsch, 2007.

[11] G.M. van der Zalm: Tuning of PID-Type Controller: Literature Overview, DCT-report nr. 2004.54, Technische Universiteit Eindhoven, 2004.

[12] Bomberg, B.C.; Hurley, P.E.; Clark, C.A.; McLaughlin, C.S.: Complications Associated with the Use of an Infusion Pump during Knee Arthroscopy, *Arthroscopy*, pp.224-228, 1992.

[13] Katsuhiko, Ogata: Modern Control Engineering, 5th Edition, Prentice Hall, 2010.

[14] Viorel, Nicolau: On PID Controller Design by Combining Pole Placement Technique with Symmetrical Optimum Criterion, Research Article on Mathematical Problems in Engineering, Hindawi Publishing Corporation, 2013.

[15] C., Kessler: “Das Symmetrische Optimum”, Regelungstechnik, vol.6, pp. 395-400 and 432-436, 1958.